Genome-wide analysis of experimentally evolved *Candida auris* reveals multiple novel mechanisms of multidrug-resistance.

Hans Carolus[a,b], Siebe Pierson[b], José F. Muñoz[c], Ana Subotić[a,b], Rita B. Cruz[b], Christina A. Cuomo[c], Patrick Van Dijck[a,b,#]

[a] VIB Center for Microbiology, Leuven, Belgium

[b] Department of Biology, KU Leuven, Leuven, Belgium

[c] Broad Institute of MIT and Harvard, Cambridge, MA, USA

[#] Address correspondence to Patrick Van Dijck, patrick.vandijck@kuleuven.vib.be

Running head: Experimental evolution of multidrug-resistance in *C. auris*

Keywords: *Candida auris*, multidrug-resistance, micro-evolution, whole genome sequencing

Abstract

Candida auris is globally recognized as an opportunistic fungal pathogen of high concern, due to its extensive multidrug-resistance (MDR). Still, molecular mechanisms of MDR are largely unexplored. This is the first account of genome wide evolution of MDR in *C. auris* obtained through serial *in vitro* exposure to azoles, polyenes and echinocandins. We show the stepwise accumulation of multiple novel mutations in genes known and unknown in antifungal drug resistance, albeit almost all new for *C. auris*. Echinocandin resistance evolved through a codon deletion in *FKS1* accompanied by a substitution in *FKS1* hot spot 3. Mutations in *ERG3* and *CIS2* further increased the echinocandin MIC. Decreased azole susceptibility was acquired through a gain of function mutation in transcription factor *TAC1b* yielding overexpression of the drug efflux pump Cdr1; a segmental duplication of chromosome 1 containing *ERG11*; and a whole chromosome 5 duplication, which contains *TAC1b*. The latter was associated with increased expression of *ERG11, TAC1b* and *CDR2*, but not *CDR1*. The simultaneous emergence of nonsense mutations in *ERG3* and *ERG11*, presumably leading to the abrogation of ergosterol synthesis, was shown to decrease amphotericin B susceptibility, accompanied with fluconazole cross resistance. A mutation in *MEC3*, a gene mainly known for its role in DNA damage homeostasis, further increased the polyene MIC. Overall, this study shows the alarming potential and diversity for MDR development in *C. auris,* even in a clade until now not associated with MDR (clade II), hereby stressing its clinical importance and the urge for future research.

Importance

C. auris is a recently discovered human fungal pathogens and has shown an alarming potential for multi- and pan-resistance towards all classes of antifungals most commonly used in the clinic. Currently, *C. auris* has been globally recognized as a nosocomial pathogen of high concern due to this evolutionary potential. So far, this is the first study in which the stepwise progression of MDR in *C. auris* is monitored *in vitro*. Multiple novel mutations in known 'resistance genes' and genes previously not or vaguely associated with drug resistance reveal rapid MDR evolution in a *C. auris* clade II isolate. Additionally, this study shows that *in vitro* experimental evolution can be a powerful tool to discover new drug resistance mechanisms, although it has its limitations.

Introduction

Over the course of a decade since its discovery (1), *Candida auris* has emerged in at least 39 countries along every inhabited continent (2), occasionally causing healthcare-associated outbreaks of lethal candidiasis (3). *C. auris* is substantially different from any other *Candida* species studied so far, as it behaves like a true multidrug-resistant (MDR) nosocomial pathogen (cfr. methicillin resistant *Staphylococcus aureus*, MRSA) (3). This was illustrated by the US Center for Disease Control and Prevention (CDC) in 2019, as they listed *C. auris* as the first fungus among urgent antimicrobial resistance threats (4). *C. auris* can become resistant to each drug and each combination of drugs from the three major antifungal drug classes: the azoles (e.g. fluconazole), echinocandins (e.g. caspofungin) and polyenes (e.g. amphotericin B).

Various clinical isolate screening reports indicate fluconazole resistance in over 80% (5-9) and amphotericin B resistance in up to 30% of the isolates tested (6, 7). Echinocandin resistance is less common, found in 2-10% in some screenings (6-8, 10), but it is alarmingly on the rise (11, 12). Overall, about 90% of the *C. auris* isolates are estimated to have acquired resistance to at least one drug, while 30-41% are resistant to two drugs, and roughly 4% are pan-resistant (resistance to the three major antifungal drug classes) (4, 7). These numbers show an unprecedented potential to acquire MDR, unlike any other pathogenic *Candida* species (3, 12, 13). The molecular mechanisms of antifungal drug resistance, especially for amphotericin B resistance and MDR, are still poorly understood in *C. auris*. Hundreds of resistant *C. auris* strains have been sequenced and their decreased drug susceptibility for azoles and echinocandins has been associated with a handful of mutations in genes known to be involved in drug resistance. Still, the high levels of resistance and extensive MDR in some strains cannot

be explained through the limited number of resistance-conferring mutations described so far (3, 7).

Azole resistance has been linked to three single nucleotide polymorphisms (SNPs) (7-9, 14) and an increased copy number (9, 15) of *ERG11*, the gene encoding the fluconazole target lanosterol 14-α-demethylase. Additionally, the ATP Binding Cassette (ABC) transporter Cdr1, was proven to act as an efflux pump of azoles in *C. auris* (16-18) and a recent study suggests that gain of function (GOF) mutations in *TAC1b* can underly this mode of action (16). Echinocandin resistance in *C. auris* was previously only linked to SNPs substituting amino acid S639 (9, 12, 19) and F635 (20) of Fks1, which is the echinocandin target: β(1,3) D-glucan synthase. The polyene amphotericin B works by sequestering ergosterol, rather than inhibiting a specific enzyme and therefore, amphotericin B resistance is among the least understood drug resistance mechanisms in *C. auris* and *Candida* sp. in general (12). So far, only an increased expression of genes involved in ergosterol biosynthesis (i.e. *ERG1, ERG2, ERG6* and *ERG16*) (15), SNPs in the gene encoding the transcription factor Flo8 and an unnamed membrane transporter encoding gene (21), had been linked to amphotericin B resistance in *C. auris* (12, 19). Overall, few studies have actually been able to validate the proposed drug resistance mechanisms in *C. auris* (16, 18, 22, 23), presumably because of the lack of an optimized gene-editing system for *C. auris*.

Here, we circumvent challenging and laborious gene-editing in *C. auris* (16, 22, 24) through a strategy of serial transfer based experimental evolution with the ability to trace back the emergence - and validate the causality - of single mutations or copy number changes throughout the evolutionary process. By designing allele specific PCR primers, the presence or absence of specific mutations could easily be screened for by PCR on multiple single clones in the daily evolving populations. Doing so, we validated 10 non-synonymous mutations in eight genes, evolved in 5 separate evolutionary lineages. When drug resistance became apparent, single clones from each lineage were whole genome sequenced and the SNPs, insertions/deletions (Indels) and copy number variants (CNVs) discovered were validated.

In this study we investigated MDR evolution in a clade II *C. auris* strain, which is understudied comparted to other clades (25) and has been suggested to be less prone to drug resistance development (25, 26). Previously, five different clades (clade I -V, i.e. the South Asian, East Asian, African, South American and Iranian clade resp.) of *C. auris* have been identified, each separated by thousands of SNPs (7, 27), and often associated with clade-specific virulence and/or drug resistance tendencies (9, 25, 26). As such, this study shows that clade II *C. auris*

can also rapidly acquire MDR *in vitro* and its mechanisms of resistance provide fundamental knowledge on how resistance can be acquired by *C. auris*. Finally, our study presents both the power and challenges of using *in vitro* experimental evolution to discover the molecular mechanisms of (multi)drug-resistance.

Results

***C. auris* clade II can acquire multidrug-resistance rapidly *in vitro*.** *C. auris* strain B11220, the original type strain described by Satoh *et al*. (1) in Japan 2009, was the only strain used for this study. A single colony isolate from strain B11220 (further referred to as wild type, wt), was subjected to an *in vitro* experimental micro-evolution assay as depicted and described in **figure 1A** and the methods section respectively. The wild type strain proved to be pan-susceptible (determined by minimum inhibitory concentration or MIC_{50}, see method section) to the three major antifungal drug classes: fluconazole MIC_{50}: 1µg/ml, caspofungin MIC_{50}: 0.125µg/ml and amphotericin B MIC_{50}: 0.5µg/ml. Based on these MIC_{50} values, the wild type strain was exposed (in triplicate) to three concentrations of each drug: $2xMIC_{50}$, $1xMIC_{50}$ and $0.5xMIC_{50}$ or no drug, representing three selective pressures and a control, respectively. Serial transfer with conditional drug treatment (**figure 1A**) was maintained for 30 days or until drug resistance became evident from regular MIC testing. An overview of the ancestry of the evolved strains is depicted in **figure 1B**.

Five strains were evolved and sequenced: F30, C20, A29, FC17 and CF16: strain B11220 (wild type) was exposed to **F**luconazole (**F**-lineage), **C**aspofungin (**C**-lineage) and **A**mphotericin B (**A**-lineage), after which the single resistant strains obtained were exposed to a second drug to acquire multidrug-resistance, yielding the **FC-** and **CF**-lineage for the **F** (**F**luconazole resistant) strain that was given **C**aspofungin and the **C** (**C**aspofungin resistant) strain that was given **F**luconazole respectively. The name of each strain represents the experimental lineage (letter which refers to the treatment/resistance), and day of isolation (number), respectively. **Figure 2** shows the MIC_{50} values for each drug and each end-point strain (F30, C20, A29, FC17 and CF16) evolved. The length of the evolution experiment ranged from 16 (CF-lineage) to 30 days (F-lineage), although later it was shown that resistant clones emerged quite early (e.g. after three days in C-lineage, see **figure 2**).

Allele-specific PCR is an effective method for tracing back the emergence of mutations during evolution in serial isolates. After micro-evolution, whole genome sequencing of the wild type strains and strain F30, C20, A29, FC17 and CF16 showed the acquisition of 10 non-

synonymous mutations (listed in **table 1**) and two different aneuploidies (shown in **figure 6**, validation shown in supplementary **figure S3**). All mutations identified were novel to *C. auris* based on literature review and comparison of sequences with a set of 304 globally distributed *C. auris* isolate sequences representing Clade I, II, III and IV (9). The impact of individual mutations and CNVs will be discussed in the following paragraphs.

To validate the causality of single mutations in strains that harbored more than one mutation, we applied a screening strategy of allele-specific PCR (AS-PCR). AS-PCR primers were designed as described by Liu *et al.* (28), implementing a specific mismatch at the third position of the 3' end of the allele-specific primer to increase specificity. An overview of the universal, and allele specific primers used to perform AS-PCR, is given in supplementary **table S1**. The specificity and sensitivity of all AS-PCR primers was assessed by performing temperature gradient PCRs on serial dilution reference DNA template (for one example see supplementary **figure S2**). Populations were re-cultured from the -80°C collection of daily stored aliquots (populations) and AS-PCR was performed on gDNA extracted from a maximum of 30 single clones of each (daily) population. After confirmation of the emergence of a mutation of interest, alleles were verified by sequencing a +-1000 bp region spanning the allele of interest. Primers used for PCR and sequencing are given in supplementary **table S1.** Next, the influence of this single mutation on the drug susceptibility was determined by performing a broth dilution assay (BDA, see Antifungal susceptibility testing in method section). **Figure 2** shows the impact of each individual mutation on the MIC for the drug of interest for each lineage evolved, except for the A-lineage, in which the mutations in *ERG3* and *ERG11* (**table 1**) was present or absent simultaneously in the 30 clones that were checked per population.

Novel mutations in *FKS1* and *ERG3* yield extensive echinocandin resistance with minor growth discrepancies. Caspofungin resistance was evolved twice in this study, once as monoresistance in the C-lineage, and once as multidrug-resistance in the FC-lineage, derived from the fluconazole resistant strain F30 (**figure 1B**). The susceptibility to caspofungin decreased drastically in both strain C20 and FC17 (MIC_{50} >64µg/ml) (**figure 2**). Whole genome sequencing revealed three mutations in the C20 strain: a missense mutation (atG/atA|M690I) and codon deletion (ttcttg/ttg|FL635L) in *FKS1* (B9J08_000964; **table 1**), the gene encoding the catalytic subunit of the echinocandin drug target β(1,3) D-glucan synthase, and one missense mutation (Cta/Ata|L207I) in *ERG3*, encoding sterol Δ5,6-desaturase (B9J08_003737; **table 1**). The exact same codon deletion (ttcttg/ttg|FL635L) in *FKS1* emerged

independently during caspofungin resistance evolution in the FC-lineage (**table 1**). Two additional mutations emerged during the evolution of strain FC17, namely a missense mutation (gAt/gTt|D367V) in the *PEA2* gene, encoding a subunit of the polarisome (B9J08_001356; **table 1**), and a missense mutation (Gca/Aca|A27T) in the *CIS2* gene, encoding a γ-glutamylcysteine synthetase (B9J08_003232; **table 1**). Tracing back the emergence of these mutations shows that the *FKS1* mutation FL635L increased the MIC_{50} of the wild type strain 500-fold: from 0.125µg/ml to 64µg/ml (**figure 2**). It is however the mutations in *CIS2* (emerged in FC16) and *ERG3* (present in C20) that further increased the caspofungin MIC_{50} to >64µg/ml (**figure 2**).

Acquired echinocandin resistance in fungi has been associated with several specific mutations in three defined 'hot spot' regions (HS) in the *FKS1* gene (29). **Figure 3** shows an amino acid sequence alignment of the *FKS1* gene HS1, HS2 and HS3 regions, constructed to compare the mutations found in this study to those known to confer echinocandin resistance in *C. auris* and other fungi as described in literature. This literature review shows that the codon deletion at position F635 as found in this study; also has been reported to confer decreased echinocandin susceptibility in *C. glabrata* (29). The same amino acid was substituted (not deleted as in C-lineage here) in echinocandin resistant *C. auris* strains reported recently (20). The *FKS1* mutation M690I is located in hot spot region 3 without comparable mutations in pathogenic fungi (**figure 3**), and seems to have no direct impact on the drug susceptibility to caspofungin in the C-lineage (**figure 2**).

Figure 4 shows the growth curves of all end-point evolved strains, plotted based on growth in RPMI-MOPS medium supplemented with 0,2% or 2% glucose (**figure 4A and 4B** respectively). From these growth plots, it is clear that caspofungin resistant strains C20 and FC17 hardly had any growth discrepancies compared to the parent wild type strain under physiological conditions, showcasing the lack of fitness trade-offs associated with the acquisition of echinocandin resistance described above.

Mutations of *ERG3*, *ERG11*, *FLO8* and *MEC3* results in amphotericin B and fluconazole resistance but impede growth. During micro-evolution, the MIC of amphotericin B increased 8-fold in the A-lineage: from IC_{50}: 0.5µg/ml (wt) to MIC_{50}: 4µg/ml in strain A29 (**figure 2**). Simultaneously, cross-resistance to fluconazole emerged, with an MIC increase from 1µg/ml to over 64µg/ml (**figure 2**). Two nonsense mutations in genes involved in the ergosterol biosynthesis pathway were found (**table 1**), namely the tgG/tgA|W182* mutation in the *ERG3*

gene and the Gag/Tag|E429* mutation in the *ERG11* gene, encoding lanosterol 14-alpha-demethylase (B9J08_001448; **table 1**). The *ERG11* mutation of strain A29 lies within a region of *ERG11* that corresponds to a frequently mutated ('hotspot') region of *ERG11* in azole resistant *C. albicans* (30, 31). It is however distinct from the three SNPs of *ERG11* (namely Y132F, K143R and F126L) that have been linked to drug (azole) resistance in *C. auris* so far (7-9, 14), and are situated in another 'hotspot' region of *ERG11* (30, 31).

Additionally, a nonsense mutation (Cag/Tag|Q384*) was found in the transcription factor *FLO8* gene (B9J08_000401, **table 1**), and a missense mutation (gCg/gTg|A272V) emerged in the *MEC3* gene which encodes a subunit part of the Rad17p-Mec3p-Ddc1p sliding clamp (B9J08_003102; **table 1**). Remarkably, the mutation in *MEC3* increased the amphotericin B resistance two-fold (from MIC_{50}:2µg/ml in strain L21 to MIC_{50}:4µg/ml in strain L27, see **figure 2**). The mutation in *FLO8* did not seem to alter the drug susceptibility for fluconazole or amphotericin B. Additionally, strain A29 was found to significantly overexpress *TAC1b* and *ERG11,* as shown by reverse transcriptase quantitative PCR (RT-qPCR), shown in **figure 5.** Observations in the lab and characterization of the growth curve showed that strain A29 was most impeded in growth, compared to the wild type strain and other evolved strains, as shown in **figure 4.**

A *TAC1b* mutation and upregulated *CDR1* expression decrease fluconazole susceptibility. In strain F13, a codon deletion (ttc/|F15) in the *TAC1b* gene was identified (B9J08_004820; **table 1**) that corresponded to a 32-fold increase in the MIC_{50} of fluconazole (**figure 2**). Tac1b is an activating transcription factor, positively regulating the expression of the ATP Binding Cassette (ABC) transporter Cdr1, known to be involved in azole efflux and azole resistance in *C. auris* (16, 22). Although the mutation in strain F13 is novel, it is located in a region of *TAC1b* that is known to harbor gain-of-function mutations in fluconazole resistant clinical isolates of *C. auris*, as shown by Rybak *et al*. (16). Nevertheless, it is the first codon deletion (cfr. SNPs) in this region suggested to confer a gain of function of *C. auris TAC1b.* Gene expression analysis of strain F12 (no *TAC1b* mutation) and strain F13 (*TAC1b* mutation obtained) confirms that this mutation increased the expression of *CDR1* (B9J08_000164) significantly, as shown in **figure 5.** The overexpression of *CDR1* is maintained in strain F30 and in the multidrug-resistant strain FC17, as shown in **figure 5.**

Two aneuploidies independently emerged during fluconazole resistance evolution. Read coverage of whole genome sequencing was used to analyze copy number variation (CNV), by

231 calculating normalized depth read coverage per 5kb window (see methods section). A visual
232 representation of this normalized coverage for each chromosome in all end-point sequenced
233 strains is displayed in **figure 6.** This reveals a segmental and whole chromosome duplication
234 emerged in the F- and CF-lineage respectively, both seemingly involved in fluconazole
235 resistance evolution.
236 The 191 kb segmental duplication of Chr1 in the F30 strain contained 75 protein encoding
237 genes (based on the B11220 reference genome annotation; CP043531-CP043537), including
238 *ERG11*. During further evolution to caspofungin in the FC-lineage (see **figure 1B**), this
239 segmental duplication was maintained but decreased in size to 161kb containing 67 protein
240 encoding genes (still including *ERG11*). The segmental Chr1 duplication resulted in an over
241 two-fold decrease in fluconazole susceptibility, increasing the MIC_{50} of 32µg/ml in strain F13
242 to MIC_{50} >64µg/ml in strain F30, as shown in **figure 2**. Expression analysis showed that the
243 duplication led to increased expression of *ERG11,* not present in strain F13 (**figure 5**). Strain
244 F30 was also marked by a slight decrease in amphotericin B susceptibility, retained in the FC17
245 strain (**figure 2**). This is possibly due to *ERG11* overexpression.
246 The whole chromosome 5 (Chr5) duplication in the CF16 strain contained a region of 933kb
247 encompassing 405 protein encoding genes, including and *TAC1b*. This aneuploidy marks the
248 difference between strain C20 and strain CF16 and is therefore suggested to confer the 32-fold
249 decrease in fluconazole susceptibility between those strains (**figure 2**). Expression analysis
250 showed that the duplication of Chr5 correlates with a significant overexpression of *TAC1b* and
251 *CDR2* (B9J08_002451), but not *CDR1* in strain CF16 (**figure 5**).
252

253 ## Discussion

254 **First, this study shows the evolution of multiple mechanisms known to be involved**
255 **in drug resistance in fungi, albeit new to *C. auris*.** In the largest screening of *C. auris* clade
256 II strains, 62.3% of a total of 61 isolates proved to be fluconazole resistant although only 3
257 isolates harbored a known azole-conferring mutation in *ERG11* (K143R) (32). This indicates
258 that other mechanisms of azole resistance play a role in *C. auris* clade II (32). Here, we describe
259 at least four molecular mechanisms, none of which include the most common mutations in
260 *ERG11*, by which fluconazole susceptibility can decrease in a clade II *C. auris* strain *in vitro*.
261 Previous reports show that many GOF mutations in *TAC1* or homologues of this transcription
262 factor can confer azole resistance in *Candida* species (33-35), including *C. auris* (16), through
263 an overexpression of the drug efflux pump Cdr1. Most GOF mutations are found in the region

encoding the putative transcriptional activation domain of *TAC1*, situated in the C-terminal portion of the protein in *Candida* sp. (36). Rybak *et al.* report one mutation in this region (codon deletion at position F862) to be associated with fluconazole resistance in *C. auris* although all other resistance associated mutations lie between the DNA binding, transcription factor and activation domain of *TAC1b* (16). One such mutation (F214S), discovered in an experimentally evolved strain of *C. auris,* lies in the proximity of the codon deletion at position 191 as we discover here. Based on these reports and our findings, we therefore hypothesize that F191Δ is a new potential gain of function mutation of *C. auris TAC1b* conferring azole resistance through *CDR1* overexpression. Nevertheless, previous reports have shown that Tac1b might function in other, Cdr1-independent ways to decrease azole susceptibility in *C. auris* (16, 22). Another mechanism of reduced azole susceptibility discovered in this study involves aneuploidies. In *C. albicans,* both *TAC1* and *ERG11* are located on Chr5, and the duplication of this region by forming an isochromosome [i(5L)] has been reported to confer azole resistance *in vitro* and *in vivo* (37). Based on this and reports on azole resistance in *C. auris* due to CNVs and/or overexpression of *ERG11* (9, 15, 38), we hypothesize a similar mode of action in strain F30. Moreover, comparing drug susceptibility between strain F13 and F30, the overexpression of *ERG11* in F30 more than doubles the fluconazole MIC_{50} compared to -the already resistant- strain F13, while it decreases the susceptibly for amphotericin B (**figure 2**). Given the fact that the duplication of *C. auris* Chr5 is the only genomic alteration that distinguishes strain CF16 from strain C20, we propose that this duplication is here too responsible for azole resistance. Expression analysis shows however, that the duplication and subsequent overexpression of *TAC1b* (**figure 5**) does not correspond to an increased expression of *CDR1,* as was expected, but *TAC1b* may play a CDR1-independent role in azole resistance of *C. auris,* as suggested by Mayr *et al.* (22).

The acquisition of resistance to polyenes is among the least understood of all antifungal drugs and has been linked to mutations in the ergosterol biosynthesis pathway in *Candida* sp. including *ERG2* (39), *ERG6* (40), *ERG11* (41) and *ERG3* (42). Cross resistance to azoles and amphotericin B has often been associated to the abrogation of two *ERG*-genes simultaneously (43). One such example is the combination of the loss of function (LOF) of *ERG11* and *ERG3* in *C. tropicalis* (44, 45). Upon the abrogation of *ERG11*, due to a LOF mutation or the action of azoles, a toxic 3,6-diol derivative is produced through the action of the sterol $\Delta^{5,6}$ desaturase, encoded by *ERG3* (46). Simultaneous disruption of the function of both *ERG3* and *ERG11* can undo this detrimental effect (43). Here we show for the first time that such a mechanism of cross-resistance can establish in *C. auris.*

298 Target alteration is the most commonly observed and most studied mechanism of
299 echinocandin resistance in *Candida* species (47). Most echinocandin resistance conferring
300 *FKS1* mutations in *C. auris* occur at position S639 (12, 19) although most recently, a SNP at
301 position F635, the same codon deleted in strain C3 in this study, was linked to resistance in the
302 clinic (20), see **figure 3**. In general, mutations in echinocandin resistant *Candida* species lie
303 within two small, strictly defined 'hot spot regions' of *FKS1* (47). However, the codon
304 substitution at position 690, emerged in strain C15 occurs in the elusive 'hot spot 3', a third
305 potent hot spot region discovered by site-directed mutagenesis of *S. cerevisiae* (29). This
306 mutation occurred after the codon deletion at position 635 (in HS1) in the C-lineage but did
307 not affect the echinocandin MIC_{50}, possible indicating functional compensation of the altered
308 Fks1 protein. A third mutation of strain C20 occurred in *ERG3*. One report shows that a
309 mutation in *ERG3* in a clinical *C. parapsilosis* strain conferred both resistance to azoles and
310 echinocandins (17). Here we observe a slight increase, rather than a decrease in fluconazole
311 susceptibility upon the emergence of the *ERG3* mutation in strain C20 (**figure 2**). Most
312 interestingly this mutation further increases the MIC_{50} for caspofungin in strain C20, compared
313 to strain C15, which only obtained *FKS1* mutations (**figure 2)**. Overall, the caspofungin
314 resistant strains (FC17, C20) show MIC values (>64µg/mL) that exceed previously reported
315 values in *C. auris* (8, 48-50). Like Rybak *et al.* (17), we therefore suggest that the underlying
316 mechanisms of echinocandin resistance in *C. auris*, including the role of *ERG3*, should be
317 further investigated.
318
319 **Four genes were mutated that were previously not or vaguely associated with drug**
320 **resistance in fungi.** *FLO8,* mutated in the amphotericin B resistant strain A29, encodes a
321 transcription factor known to be essential for filamentation *C. albicans* (51). This filamentation
322 was shown to decrease the rate of programmed cell death in *C. albicans*, when exposed to
323 amphotericin B (52). Flo8 has multiple downstream effects, one of which is the positive
324 regulation of *ERG11* expression shown in *S. cerevisiae* (53) and thus potentially playing a role
325 in azole and amphotericin B resistance. In a recent study of clinical *C. auris* isolates from
326 South-America, a non-synonymous mutation in the *FLO8* gene significantly correlated to
327 amphotericin B resistance (21). In a follow-up study on the structure of FLO8, the authors
328 suggest a potential role of FLO8 in *C. auris* virulence and drug resistance, arguing that the
329 *FLO8* mutation found before (21), could be a gain of function mutation (54). In our study
330 however, we see a nonsense mutation, abrogating Flo8 at amino acid 100, assuming to be
331 disruptive to its function. Earlier, a LOF of *FLO8* was found to play a role in azole resistance

with a *FLO8* deletion correlated to increased *TAC1, CDR1* and *CDR2* expression and azole resistance, while *FLO8* overexpression lead to decreased *CDR1* expression (55). Although these reports strengthen the suspicion of a role of Flo8 in drug resistance, we cannot validate the influence on the resistance phenotype of the nonsense mutation observed here. Further research on Flo8 in drug resistance is therefore highly desirable.

The fourth gene mutated during amphotericin B resistance evolution is an ortholog of *MEC3*, encoding a DNA damage checkpoint protein as part of the Rad17p-Mec3p-Ddc1p sliding clamp, involved primarily in DNA damage recognition and repair in *S. cerevisiae* (56). No clear reports of a function for *MEC3* in antifungal drug resistance were found, although two studies mention the upregulation of *MEC3* upon the acquisition of azole resistance in an experimentally evolved *C. glabrata* strain (35, 57). Our results show that the mutation in *MEC3* has a significant influence on susceptibility to amphotericin B, doubling the MIC_{50} (**figure 2**). The mechanism behind increased amphotericin B resistance upon acquiring a mutation in *MEC3*, remains unclear.

Strain FC17 harbored a mutation in *CIS2,* of which the *S. cerevisiae* ortholog (*ECM38*) encodes a γ-glutamyltranspeptidase, involved in glutathione degradation (58), detoxification of xenobiotics (59), and cell wall biogenesis (60). The role *CIS2* plays in the latter, regarding echinocandin resistance, remains unclear but as for the former, a study from Maras and colleagues (61) illustrated that fluconazole and micafungin resistance was accompanied by altered levels of glutathione in *C. albicans*, hypothesized to counteract oxidative stress caused by these antifungal drugs. In that study, the increased levels of glutathione were accompanied by the overexpression of γ-glutamylcysteine synthetase (61). A role for *CIS2* and glutathione catabolism, in drug resistance mediated by an altered redox metabolism remains to be elucidated.

The fourth mutation in the FC-lineage lays within a gene predicted to encode *PEA2*, a subunit of the polarisome, involved in polarized growth and morphogenesis in *S. cerevisiae* (62). This mutation has however no significant effect on the drug resistance profile and might thus be the result of random genetic drift.

Experimental evolution can be a powerful tool to research resistance, although it has limitations. Due to recent advances in next generation sequencing technology, genome-wide studies of drug resistance have become more common (63, 64). The classic approach of sequencing drug resistant clinical isolates directly from patients (63) has many limitations,

365 including the often unavailability of the original genotype and the difficulty to resolve
366 mutations associated with drug resistance from those that have accumulated due to host-
367 pathogen interactions. *In vitro* experimental evolution copes with most of these problems (63,
368 65), is highly repeatable and allows controlled long term monitoring of different strains and
369 conditions. Moreover, the ability to isolate and investigate each generation separately, allows
370 to monitor both the speed and the stepwise progression of drug resistance development.
371 Nevertheless, *in vitro* experimental evolution has its own limitations, such as the homogeneity
372 of the selective pressure in the absence of metabolization of the drug, tissue specific exposure
373 and host-pathogen interactions. However, studies of antifungal drug resistance by *in vitro*
374 evolution often resemble acquired resistance found in clinical isolates (63, 65). In regards to
375 our results, a comparative analysis of mutations reported in literature and re-analysis of variants
376 predicted in 304 sequenced clinical isolates of *C. auris* (9), show that most mechanisms of drug
377 resistance proposed here are novel. One must be careful by redeeming these findings to be
378 nonrelevant to the *in vivo* setting or clinical environment, reports on resistance mutations
379 (providing whole genome analysis) is still scarce and the data base of 304 sequenced clinical
380 isolates of *C. auris* (9) is still limited, with only 23% of isolates reported multidrug-resistant
381 and only include 7 clinical isolates that belong to clade II (6 isolates pan-susceptible, 1 isolate
382 fluconazole resistant) (9). This and other studies in bacteria (66) and fungi (13, 65, 67) show
383 that *in vitro* experimental evolution can be a powerful tool, especially if combined with an
384 effective approach to trace the full evolutionary history of mutation events, as we did here
385 using allele-specific PCR screening
386
387 ***Candida auris* clade II is, like most other *C. auris* clades, exceptionally capable of**
388 **MDR development.** Clade II *C. auris* is one of the least studied clades (25) and this report
389 aids to close this research gap. In general, few phenotypic differences have been characterized
390 that differentiate the five *C. auris* clades from one another, although collected isolates vary
391 substantially in the frequency of drug resistance between clades and mutations identified (9,
392 15). More research should be performed identify clade specific phenotypes or evolutionary
393 tendencies, to anticipate on geographically defined emergence and outbreaks in the field.
394 Overall, *C. auris* is still significantly understudied, compared to other *Candida* species such as
395 *C. albicans* and *C. glabrata,* despite the fact that it is an urgent antimicrobial resistant threat
396 (4). Further fundamental knowledge on how *C. auris* can thrive as “nosocomial MDR fungus”
397 is highly needed to efficiently tackle this pathogen in the future.

Materials and methods

Strains and growth conditions

All experiments were performed with *C. auris* strain B11220 (CBS10913) from the Westerdijk Fungal Biodiversity Center (wi.knaw.nl/). Strains were grown on YPD agar (2% glucose) at 37°C and enriched in RPMI – MOPS liquid medium containing 2% glucose at 37°C in a shaking incubator overnight. All strains, including daily aliquots of serially transferred populations in the micro-evolution assay, were stored at -80°C in RPMI – MOPS medium containing 25% glycerol.

Antifungal susceptibility testing

The Minimal Inhibitory Concentration (MIC) was determined by a broth dilution assay (BDA) according to Clinical and Laboratory Standards Insititute (CLSI) guidelines (68). In short, a dilution of 64µg/ml to 0.06 µg/ml of each drug was prepared in RPMI-MOPS medium in a 96-well polystyrene microtiter plate. A standardized amount of 100 to 500 cells was dissolved in a final volume of 200µL per well and plates were incubated at 37°C. Growth was measured after 48h of incubation through spectrophotometric quantification of OD_{600} in a SPECTRAmax® Plus 384 microplate reader (Molecular Devices). Minimal Fungicidal Concentration (MFC) was determined by spotting the resuspended 96-well microtiter plate content on YPD agar (2% glucose) and incubation for 48h. Resistance is determined through tentative breakpoints provided by the CDC (6).

In vitro experimental evolution assay

An overview of the design of the experimental evolution assay is given in figure 1A. At the start of the evolution experiment, 10^6 cells are diluted in a 5ml volume of RPMI-MOPS medium (2% glucose) containing no drug (control) or a drug at a concentration of $1/2xMIC_{50}$, $1xMIC_{50}$ or $2xMIC_{50}$. All conditions were performed in triplicate (3 evolving populations per condition). After 24h of incubation at 37°C in a shaking incubator, growth of each population was compared to the average growth of 3 controls (no drug) by spectrophotometric quantification (OD_{600}). Next, 500µL of each population was transferred to 4500µL of fresh medium with a concentration of drug equal to the previous culture when OD_{600} [evolving population] $\leq$ OD_{600} [average control] or double to the previous culture when OD_{600} [evolving population] > OD_{600} [average control]. The experiment was terminated after 30 days or if the MIC_{50} exceeded the resistance breakpoint value, as evaluated by intermediate MIC testing.

Analysis of growth

Growth was assessed by spectrophotometric observation (OD_{595}) over time in a Multiskan™ GO (Thermo Scientific) automated plate reader using flat bottom 96-well plates and intermitted (30 min. interval) pulsed shaking (medium strength, 5 min). Cultures were diluted in RPMI-MOPS medium containing 0.2% or 2% glucose, to a final volume of 10^6 cells per well. Growth was measured for 72h at 37°C. Growth curves were plotted as an average values of 3 biological repeats with 3 technical repeats per biological repeat.

DNA extraction

Genomic DNA for whole genome sequencing was extracted using the MasterPure™ Yeast DNA Purification kit (Lucigen, US) following the manufacturers protocol. For (AS-)PCR and sanger sequencing, DNA was isolated from the cells through phenol chloroform isoamyl alcohol (PCI) extraction. Cells were dissolved in 300µL Tris EDTA (TE) buffer with 300µL PCI solution (phenol pH 6.7 – chloroform – isoamylalcohol 25:24:1) and lysed by micro-bead shearing in a 'fast prep' centrifuge (20 sec, 6m/sec)(MP biomedical™). After cell lysis, DNA was isolated and purified using ethanol precipitation. The resulting DNA was diluted to a concentration of 200ng/µL in milliQ H_2O, based on the DNA concentration measured through absorbance at 260 nm with a NanoDrop spectrophotometer (Isogen).

Whole genome sequencing and analysis

Genomic libraries were created using the NEBNext® Ultra DNA library Prep Kit for Illumina sequencing (New England Biolabs, US) and genomes were sequenced on an Illumina MiSeq v2 500 (Illumina, US) obtaining a coverage of at least 50x. Standard quality control was performed using FastQC v0.11.7 (69). Paired end reads were aligned using BWA mem v0.7.17 (70) to the annotated genome assemblies of strain B8441 [clade I; Genbank: GCA_002759435.2 (15)] and B11220 [clade II; Genbank: CP043531-CP043537 (26)] . For SNP and Indel identification, the assembly alignment to the annotated genome of strain B8441 (clade I) was used, while CNV analysis was performed using the assembly alignment to reference genome B11220 (clade II) respectively. The genome sequences of all end-point experimentally evolved strains were deposited to NCBI sequencing read archive (SRA) under "BioProject PRJNA664007". Variants were identified and filtered using GATK v4.1.2.1 (71, 72), with the haploid mode, and including GATK tools HaplotypeCaller and Variant Filtration using "QD < 2.0 ‖ FS > 60.0 ‖ MQ < 40.0". In addition, variants were filtered if they have

minimum genotype (GT) quality < 50, Alternate Allele Frequency < 0.8, or allelic depth (DP) < 10. The final VCF was annotated using SnpEff v4.3T (73). CNVs were identified using CNVnator v0.3 (74), selecting for 1kb genomic windows of significant (p<0.01) variation in normalized coverage. The average depth per 5kb window was normalized to the coverage of the whole genome sequence for each isolate and plotted in R (75). Candidate variants were compared with a set of 304 globally distributed *C. auris* isolates representing Clade I, II, III and IV (9).

PCR and Sanger sequencing

Primers for PCR and Sanger sequencing were designed *in silico* using CLC Genomics Workbench v20.0.3 (digitalinsights.qiagen.com). Primer design was based on B11220 WGS consensus sequences of the regions of interest and sequences of the genes of interest in reference genome *C. auris* B8441 downloaded from the Candida genome database (candidagenome.org). Sequencing primers were designed to include a +/-1000 region of interest (spanning the region with the mutation of interest). All primers are given in **table S1**. Amplification of regions of interest was achieved through PCR using Q5 high-fidelity DNA polymerase (New England Biolabs Inc.). The total reaction volume of 50µL consisted of the 200ng/µL DNA extract, 5µL dNTPs (0.2mM), 10µL Q5 buffer, 0,5µL Q5 polymerase (2 units), milliQ, and 0,4µL of both forward and reverse primer (1 µM). The PCR program consisted of initial denaturation at 98°C for 3 sec, 30 cycles of 98°C for 15 sec, 56°C for 25 sec, 72°C for 2 min and a final elongation step at 72°C for 2 min in a Labcycler Basic thermocycler (Bioké). Correct amplification was verified by performing electrophoresis on a 1% agarose gel at 135V for 25 min. After verification, the sequencing primers (10µM) were added to PCR amplicons and the DNA was sequenced using Sanger sequencing by Eurofins (GATC, Germany).

Allele-specific PCR (AS-PCR)

The emergence of SNPs and Indels was traced back in whole populations and a maximum of 30 single clones (colonies) per population, using a rapid sequencing free method: allele-specific SNP-PCR. Two primer pairs per gene of interest were designed according to Liu *et al.* (28), consisting of one universal primer or and one mutant-allele primer or wild type-allele primer respectively. Primers consist of an allele specific region at the 3' terminal nucleotide of the mutant or wild type allele specific primer. Additionally, a mismatch at the 3th nucleotide

from the 3' terminal was included to increase annealing specificity (28). All primers used for AS-PCR are listed in **table S1**.

To validate primer specificity, a temperature gradient PCR was performed in which annealing temperature varied between 60°C and 70°C. AS-PCR sensitivity was assessed by performing PCR on serial dilution of reference DNA template. All PCR reactions were performed in a total reaction volume of 20µL consisted of 1µL of 1/20 dilution of the pure PCI DNA extract, 5µL dNTPs (0.2mM), 10µL TaqE buffer, 0,5µL TaqE polymerase (2 units), milliQ, and 0,4µL of both forward and reverse primer (1 µM). The PCR program consisted of initial denaturation at 98°C for 3 sec, 30 cycles of 98°C for 15 sec, 56°C for 25 sec, 72°C for 2 min and a final elongation step at 72°C for 2 min in a Labcycler Basic thermocycler (Bioké). Amplification and thus the presence or absence of a mutation was verified by performing electrophoresis on a 1% agarose gel at 135V for 25 min.

Gene expression and copy number variation analysis

C. auris cells from a single colony grown overnight on YPD agar (2% glucose) were enriched in RPMI-MOPS (2% glucose) medium for 16h. These cultures were diluted to 10^8 cells in a volume of 50ml fresh RPMI-MOPS (2% glucose) medium and incubated for 8h at 37°C in a shaking incubator to ensure the harvested cells are growing in the exponential growth phase. Next, cells were harvested by centrifugation, washing in ice cold PBS, snap freezing in liquid nitrogen and stored at -80°C.

For gene expression analysis (RNA extraction and RT-qPCR), cells were resuspended in 1ml trizol and lysed by micro-bead shearing in a 'fast prep' centrifuge (20 sec, 6m/sec)(MP biomedical™). Nucleotides were extracted by washing the lysate supernatant with chloroform (360µL) and isopropanol (350µL) and precipitated by washing three times with 70% ethanol. Nucleotide concentrations and purity were measured spectrophotometrically using a NanoDrop ND-1000 (Isogen Life Science). Extracts were diluted to 1µg pure nucleotide concentration and purified by DNase treatment (New England Biolabs). cDNA was synthesized from RNA by using the iScript cDNA synthesis kit (Bio-Rad) according to the manufacturer's recommendations. Real Time qPCR was performed using GoTaq polymerase (Promega) and the StepOnePlus real-time PCR thermocycler (ThermoFisher) as follows: activation at 95°C for 2 min, 40 cycles of denaturation at 95°C for 3 seconds and annealing/extension at 60°C for 30 seconds. Primers used for qPCR were designed with the PrimerQuest tool of IDT (https://eu.idtdna.com/Primerquest/) and are listed in **table S1**. A total of 8 housekeeping genes involved in various cellular processes were assessed, of which the 3 most stable candidates

were used in the analysis (*ACT1*, *LSC2*, *UBC4*). Gene expression analysis was performed using qBasePlus software. Fold Change (with SD) was plotted from $\log_2(Y)$ transformed data and compared statistically (using a one-way ANOVA with multiple comparisons in respect to wt) with GraphPad Prism. Expression analysis in each strain was performed using 3 biological repeats each represented by the average of 2 technical repeats.

For copy number variation analysis, gDNA was extracted as described in 'DNA extraction' of methods section and standardized concentrations of 0.5 ng/µL of gDNA were used to quantify target markers (*TAC1b* and *ERG11* respectively) by qPCR using the same primers, protocol and analysis as described above.

Acknowledgement

This work was supported by an FWO personal research grant nr. 11D7620N awarded to H.C. A travel grant awarded by FWO allowed a fruitful research stay of H.C. at Broad Institute (Boston, US). C.A.C and J.F.M. were supported by the National Institute of Allergy and Infectious Diseases, National Institutes of Health, Department of Health and Human Services, under award U19AI110818 to the Broad Institute. We want to thank the group of prof. Steenackers (KULeuven) for their advice on experimental evolution.

References

1. Satoh K, Makimura K, Hasumi Y, Nishiyama Y, Uchida K, Yamaguchi H. 2009. *Candida auris* sp. nov., a novel ascomycetous yeast isolated from the external ear canal of an inpatient in a Japanese hospital. Microbiol Immunol 53:41-4.
2. Kean R, Brown J, Gulmez D, Ware A, Ramage G. 2020. *Candida auris*: a decade of understanding of an enigmatic pathogenic yeast. J Fungi (Basel) 6.
3. Forsberg K, Woodworth K, Walters M, Berkow EL, Jackson B, Chiller T, Vallabhaneni S. 2019. *Candida auris*: The recent emergence of a multidrug-resistant fungal pathogen. Med Mycol 57:1-12.
4. CDC. 2019. Antibiotic Resistance Threats in the United States, 2019, *on* U.S. Department of Health and Human Services, CDC. Accessed 26/03/20.
5. Magobo RE, Corcoran C, Seetharam S, Govender NP. 2014. *Candida auris*-associated candidemia, South Africa. Emerg Infect Dis 20:1250-1.
6. CDC. 2020. *C. auris* - Antifungal susceptibility testing and interpretation, *on* U.S. Department of Health & Human Services. https://www.cdc.gov/fungal/candida-auris/c-auris-antifungal.html. Accessed 26/03/20.
7. Lockhart SR, Etienne KA, Vallabhaneni S, Farooqi J, Chowdhary A, Govender NP, Colombo AL, Calvo B, Cuomo CA, Desjardins CA, Berkow EL, Castanheira M, Magobo RE, Jabeen K, Asghar RJ, Meis JF, Jackson B, Chiller T, Litvintseva AP. 2017. Simultaneous emergence of multidrug-resistant *Candida auris* on 3 continents confirmed by whole-genome sequencing and epidemiological analyses. Clin Infect Dis 64:134-140.

8. Chowdhary A, Prakash A, Sharma C, Kordalewska M, Kumar A, Sarma S, Tarai B, Singh A, Upadhyaya G, Upadhyay S, Yadav P, Singh PK, Khillan V, Sachdeva N, Perlin DS, Meis JF. 2018. A multicentre study of antifungal susceptibility patterns among 350 *Candida auris* isolates (2009-17) in India: role of the *ERG11* and *FKS1* genes in azole and echinocandin resistance. J Antimicrob Chemother 73:891-899.
9. Chow NA, Muñoz JF, Gade L, Berkow E, Li X, Welsh RM, Forsberg K, Lockhart SR, Adam R, Alanio A, Alastruey-Izquierdo A, Althawadi S, Belén Araúz A, Ben-Ami R, Bharat A, Calvo B, Desnos-Ollivier M, Escandón P, Gardam D, Gunturu R, Heath CH, Kurzai O, Martin R, Litvintseva AP, Cuomo CA. 2020. Tracing the evolutionary history and global expansion of *Candida auris* using population genomic analyses. mBio doi:10.1128/mBio.03364-19.
10. Bishop L, Cummins M, Guy R, Hoffman P, Jeffery K, Jeffery-Smith A, Brown C. 2017. Guidance for the laboratory investigation, management and infection prevention and control for cases of *Candida auris*. Public Health England Updated August.
11. Kathuria S, Singh PK, Sharma C, Prakash A, Masih A, Kumar A, Meis JF, Chowdhary A. 2015. Multidrug-resistant *Candida auris* misidentified as *Candida haemulonii*: characterization by matrix-assisted laser desorption ionization-time of flight mass spectrometry and DNA sequencing and its antifungal susceptibility profile variability by Vitek 2, CLSI broth microdilution, and Etest method. J Clin Microbiol 53:1823-30.
12. Lockhart SR. 2019. *Candida auris* and multidrug resistance: Defining the new normal. Fungal Genet Biol 131:103243.
13. Ksiezopolska E, Gabaldon T. 2018. Evolutionary emergence of drug resistance in *Candida* opportunistic pathogens. Genes (Basel) 9.
14. Healey KR, Kordalewska M, Jimenez Ortigosa C, Singh A, Berrio I, Chowdhary A, Perlin DS. 2018. Limited *ERG11* mutations identified in isolates of *Candida auris* directly contribute to reduced azole susceptibility. Antimicrob Agents Chemother 62.
15. Muñoz JF, Gade L, Chow NA, Loparev VN, Juieng P, Berkow EL, Farrer RA, Litvintseva AP, Cuomo CA. 2018. Genomic insights into multidrug-resistance, mating and virulence in *Candida auris* and related emerging species. Nat Commun 9:5346.
16. Rybak JM, Muñoz JF, Barker KS, Parker JE, Esquivel BD, Berkow EL, Lockhart SR, Gade L, Palmer GE, White TC, Kelly SL, Cuomo CA, Rogers PD. 2020. Mutations in *TAC1B*: a novel genetic determinant of clinical fluconazole resistance in *Candida auris*. mBio 11.
17. Rybak JM, Dickens CM, Parker JE, Caudle KE, Manigaba K, Whaley SG, Nishimoto AT, Luna-Tapia A, Roy S, Zhang Q, Barker KS, Palmer GE, Sutter TR, Homayouni R, Wiederhold NP, Kelly SL, Rogers PD. 2017. Loss of C-5 sterol desaturase activity results in increased resistance to azole and echinocandin antifungals in a clinical isolate of *Candida parapsilosis*. Antimicrob Agents Chemother 61.
18. Kim SH, Iyer KR, Pardeshi L, Munoz JF, Robbins N, Cuomo CA, Wong KH, Cowen LE. 2019. Genetic analysis of *Candida auris* implicates Hsp90 in morphogenesis and azole tolerance and Cdr1 in azole resistance. mBio 10.
19. Chaabane F, Graf A, Jequier L, Coste AT. 2019. Review on antifungal resistance mechanisms in the emerging pathogen *Candida auris*. Front Microbiol 10:2788.
20. Sharma D, Paul RA, Chakrabarti A, Bhattacharya S, Soman R, Shankarnarayan SA, Chavan D, Das P, Kaur H, Ghosh A. 2020. Caspofungin resistance in *Candia auris* due to mutations in *Fks1* with adjunctive role of chitin and key cell wall stress response pathway genes doi:https://doi.org/10.1101/2020.07.09.196600, BioRxiv.
21. Escandon P, Chow NA, Caceres DH, Gade L, Berkow EL, Armstrong P, Rivera S, Misas E, Duarte C, Moulton-Meissner H, Welsh RM, Parra C, Pescador LA, Villalobos N, Salcedo S, Berrio I, Varon C, Espinosa-Bode A, Lockhart SR, Jackson BR,

Litvintseva AP, Beltran M, Chiller TM. 2019. Molecular epidemiology of *Candida auris* in Colombia reveals a highly related, countrywide colonization with regional patterns in amphotericin B resistance. Clin Infect Dis 68:15-21.

22. Mayr EM, Ramirez-Zavala B, Kruger I, Morschhauser J. 2020. A zinc cluster transcription factor contributes to the intrinsic fluconazole resistance of *Candida auris*. mSphere 5.
23. Rybak JM, Doorley LA, Nishimoto AT, Barker KS, Palmer GE, Rogers PD. 2019. Abrogation of triazole resistance upon deletion of *CDR1* in a clinical isolate of *Candida auris*. Antimicrob Agents Chemother 63.
24. Grahl N, Demers EG, Crocker AW, Hogan DA. 2017. Use of RNA-protein complexes for genome editing in non-albicans *Candida* species. mSphere 2.
25. Welsh RM, Sexton DJ, Forsberg K, Vallabhaneni S, Litvintseva A. 2019. Insights into the unique nature of the East Asian clade of the emerging pathogenic yeast *Candida auris*. J Clin Microbiol 57.
26. Muñoz JF, Welsh RM, Shea T, Batra D, Gade L, Litvintseva AP, Cuomo CA. 2019. Chromosomal rearrangements and loss of subtelomeric adhesins linked to clade-specific phenotypes in *Candida auris* doi:https://doi.org/10.1101/754143, BioRxiv.
27. Chow NA, de Groot T, Badali H, Abastabar M, Chiller TM, Meis JF. 2019. Potential fifth clade of *Candida auris*, Iran, 2018. Emerg Infect Dis 25:1780-1781.
28. Liu J, Huang S, Sun M, Liu S, Liu Y, Wang W, Zhang X, Wang H, Hua W. 2012. An improved allele-specific PCR primer design method for SNP marker analysis and its application. Plant Methods 8:34.
29. Johnson ME, Katiyar SK, Edlind TD. 2011. New Fks hot spot for acquired echinocandin resistance in *Saccharomyces cerevisiae* and its contribution to intrinsic resistance of Scedosporium species. Antimicrob Agents Chemother 55:3774-81.
30. Marichal P, Koymans L, Willemsens S, Bellens D, Verhasselt P, Luyten W, Borgers M, Ramaekers F, Odds FC, Bossche Vande H. 1999. Contribution of mutations in the cytochrome P450 14α-demethylase (Erg11p, Cyp51p) to azole resistance in *Candida albicans*. Microbiology 145:2701-2713.
31. Wang H, Kong F, Sorrell TC, Wang B, McNicholas P, Pantarat N, Ellis D, Xiao M, Widmer F, Chen SCA. 2009. Rapid detection of *ERG11* gene mutations in clinical *Candida albicans* isolates with reduced susceptibility to fluconazole by rolling circle amplification and DNA sequencing. BMC microbiology 9:167.
32. Kwon YJ, Shin JH, Byun SA, Choi MJ, Won EJ, Lee D, Lee SY, Chun S, Lee JH, Choi HJ, Kee SJ, Kim SH, Shin MG. 2019. *Candida auris* clinical isolates from South Korea: identification, antifungal susceptibility, and genotyping. J Clin Microbiol 57.
33. Coste A, Selmecki A, Forche A, Diogo D, Bougnoux ME, d'Enfert C, Berman J, Sanglard D. 2007. Genotypic evolution of azole resistance mechanisms in sequential *Candida albicans* isolates. Eukaryot Cell 6:1889-904.
34. Coste A, Karababa M, Ischer F, Bille J, Sanglard D. 2004. *TAC1*, transcriptional activator of CDR genes, is a new transcription factor involved in the regulation of *Candida albicans* ABC transporters *CDR1* and *CDR2*. Eukaryot Cell 3:1639-52.
35. Vermitsky JP, Earhart KD, Smith WL, Homayouni R, Edlind TD, Rogers PD. 2006. Pdr1 regulates multidrug resistance in *Candida glabrata*: gene disruption and genome-wide expression studies. Mol Microbiol 61:704-22.
36. Sanglard D, Coste A, Ferrari S. 2009. Antifungal drug resistance mechanisms in fungal pathogens from the perspective of transcriptional gene regulation. FEMS Yeast Research 9:1029-1050.

37. Selmecki A, Gerami-Nejad M, Paulson C, Forche A, Berman J. 2008. An isochromosome confers drug resistance *in vivo* by amplification of two genes, *ERG11* and *TAC1*. Mol Microbiol 68:624-41.
38. Bhattacharya S, Holowka T, Orner EP, Fries BC. 2019. Gene duplication associated with increased fluconazole tolerance in *Candida auris* cells of advanced generational age. Scientific reports 9:1-13.
39. Hull CM, Bader O, Parker JE, Weig M, Gross U, Warrilow AG, Kelly DE, Kelly SL. 2012. Two clinical isolates of *Candida glabrata* exhibiting reduced sensitivity to amphotericin B both harbor mutations in *ERG2*. Antimicrob Agents Chemother 56:6417-21.
40. Vandeputte P, Tronchin G, Berges T, Hennequin C, Chabasse D, Bouchara JP. 2007. Reduced susceptibility to polyenes associated with a missense mutation in the *ERG6* gene in a clinical isolate of *Candida glabrata* with pseudohyphal growth. Antimicrob Agents Chemother 51:982-90.
41. Hull CM, Parker JE, Bader O, Weig M, Gross U, Warrilow AG, Kelly DE, Kelly SL. 2012. Facultative sterol uptake in an ergosterol-deficient clinical isolate of *Candida glabrata* harboring a missense mutation in *ERG11* and exhibiting cross-resistance to azoles and amphotericin B. Antimicrob Agents Chemother 56:4223-32.
42. Sanglard D, Ischer F, Parkinson T, Falconer D, Bille J. 2003. *Candida albicans* mutations in the ergosterol biosynthetic pathway and resistance to several antifungal agents. Antimicrob Agents Chemother 47:2404-12.
43. Sanglard D. 2016. Emerging threats in antifungal-resistant fungal pathogens. Front Med (Lausanne) 3:11.
44. Eddouzi J, Parker JE, Vale-Silva LA, Coste A, Ischer F, Kelly S, Manai M, Sanglard D. 2013. Molecular mechanisms of drug resistance in clinical *Candida* species isolated from Tunisian hospitals. Antimicrob Agents Chemother 57:3182-93.
45. Vincent BM, Lancaster AK, Scherz-Shouval R, Whitesell L, Lindquist S. 2013. Fitness trade-offs restrict the evolution of resistance to amphotericin B. PLoS Biol 11:e1001692.
46. Kelly SL, Lamb DC, Corran AJ, Baldwin BC, Kelly DE. 1995. Mode of action and resistance to azole antifungals associated with the formation of 14 alpha-methylergosta-8,24(28)-dien-3 beta,6 alpha-diol. Biochem Biophys Res Commun 207:910-5.
47. Perlin DS. 2015. Mechanisms of echinocandin antifungal drug resistance. Ann N Y Acad Sci 1354:1-11.
48. Biagi MJ, Wiederhold NP, Gibas C, Wickes BL, Lozano V, Bleasdale SC, Danziger L. Development of high-level echinocandin resistance in a patient with recurrent *Candida auris* candidemia secondary to chronic candiduria, p ofz262. *In* (ed), Oxford University Press US,
49. Kordalewska M, Lee A, Park S, Berrio I, Chowdhary A, Zhao Y, Perlin DS. 2018. Understanding echinocandin resistance in the emerging pathogen *Candida auris*. Antimicrobial agents and chemotherapy 62.
50. O'Brien B, Liang J, Chaturvedi S, Jacobs J, Chaturvedi V. 2020. Pan-resistant *Candida auris*: New York Sub-cluster Susceptible to Antifungal Combinations. BioRxiv doi:https://doi.org/10.1101/2020.06.08.136408.
51. Cao F, Lane S, Raniga PP, Lu Y, Zhou Z, Ramon K, Chen J, Liu H. 2006. The Flo8 transcription factor is essential for hyphal development and virulence in *Candida albicans*. Mol Biol Cell 17:295-307.
52. Laprade DJ, Brown MS, McCarthy ML, Ritch JJ, Austriaco N. 2016. Filamentation protects *Candida albicans* from amphotericin B-induced programmed cell death via a mechanism involving the yeast metacaspase, *MCA1*. Microb Cell 3:285-292.

53. Woods K, Hofken T. 2016. The zinc cluster proteins Upc2 and Ecm22 promote filamentation in *Saccharomyces cerevisiae* by sterol biosynthesis-dependent and -independent pathways. Mol Microbiol 99:512-27.
54. Misas E, Escandon P, McEwen JG, Clay OK. 2019. The LUFS domain, its transcriptional regulator proteins, and drug resistance in the fungal pathogen *Candida auris*. Protein Sci 28:2024-2029.
55. Li WJ, Liu JY, Shi C, Zhao Y, Meng LN, Wu F, Xiang MJ. 2019. *FLO8* deletion leads to azole resistance by upregulating *CDR1* and *CDR2* in *Candida albicans*. Res Microbiol 170:272-279.
56. Majka J, Burgers PM. 2003. Yeast Rad17/Mec3/Ddc1: a sliding clamp for the DNA damage checkpoint. Proc Natl Acad Sci U S A 100:2249-54.
57. Tsai HF, Sammons LR, Zhang X, Suffis SD, Su Q, Myers TG, Marr KA, Bennett JE. 2010. Microarray and molecular analyses of the azole resistance mechanism in *Candida glabrata* oropharyngeal isolates. Antimicrob Agents Chemother 54:3308-17.
58. Kumar C, Sharma R, Bachhawat AK. 2003. Utilization of glutathione as an exogenous sulfur source is independent of gamma-glutamyl transpeptidase in the yeast *Saccharomyces cerevisiae*: evidence for an alternative gluathione degradation pathway. FEMS Microbiol Lett 219:187-94.
59. Ubiyvovk VM, Blazhenko OV, Gigot D, Penninckx M, Sibirny AA. 2006. Role of gamma-glutamyltranspeptidase in detoxification of xenobiotics in the yeasts *Hansenula polymorpha* and *Saccharomyces cerevisiae*. Cell Biol Int 30:665-71.
60. Lussier M, White AM, Sheraton J, di Paolo T, Treadwell J, Southard SB, Horenstein CI, Chen-Weiner J, Ram AF, Kapteyn JC, Roemer TW, Vo DH, Bondoc DC, Hall J, Zhong WW, Sdicu AM, Davies J, Klis FM, Robbins PW, Bussey H. 1997. Large scale identification of genes involved in cell surface biosynthesis and architecture in *Saccharomyces cerevisiae*. Genetics 147:435-50.
61. Maras B, Angiolella L, Mignogna G, Vavala E, Macone A, Colone M, Pitari G, Stringaro A, Dupre S, Palamara AT. 2014. Glutathione metabolism in *Candida albicans* resistant strains to fluconazole and micafungin. PLoS One 9:e98387.
62. Song Q, Johnson C, Wilson TE, Kumar A. 2014. Pooled segregant sequencing reveals genetic determinants of yeast pseudohyphal growth. PLoS Genet 10:e1004570.
63. Robbins N, Caplan T, Cowen LE. 2017. Molecular Evolution of Antifungal Drug Resistance. Annu Rev Microbiol 71:753-775.
64. Sanglard D. 2019. Finding the needle in a haystack: Mapping antifungal drug resistance in fungal pathogen by genomic approaches. PLoS Pathog 15:e1007478.
65. Pais P, Galocha M, Viana R, Cavalheiro M, Pereira D, Teixeira MC. 2019. Microevolution of the pathogenic yeasts *Candida albicans* and *Candida glabrata* during antifungal therapy and host infection. Microb Cell 6:142-159.
66. Lukacisinova M, Bollenbach T. 2017. Toward a quantitative understanding of antibiotic resistance evolution. Curr Opin Biotechnol 46:90-97.
67. Fisher KJ, Lang GI. 2016. Experimental evolution in fungi: An untapped resource. Fungal Genet Biol 94:88-94.
68. Wayne P, CLSI. 2008. Reference Method for Broth Dilution Antifungal Susceptibility Testing of Yeasts; Approved Standard—Third Edition. CLSI document M27-A3. 28.
69. Andrews S. 2010. FastQC, Babraham Bioinformatics, http://www.bioinformatics.babraham.ac.uk/projects/fastqc/.
70. Li H. 2013. Aligning sequence reads, clone sequences and assembly contigs with BWA-MEM, arXiv:1303.3997 https://arxiv.org/abs/1303.3997.

766 71. DePristo MA, Banks E, Poplin R, Garimella KV, Maguire JR, Hartl C, Philippakis AA,
767 Del Angel G, Rivas MA, Hanna M. 2011. A framework for variation discovery and
768 genotyping using next-generation DNA sequencing data. Nature genetics 43:491.
769 72. McKenna A, Hanna M, Banks E, Sivachenko A, Cibulskis K, Kernytsky A, Garimella
770 K, Altshuler D, Gabriel S, Daly M, DePristo MA. 2010. The Genome Analysis Toolkit:
771 a MapReduce framework for analyzing next-generation DNA sequencing data.
772 Genome Res 20:1297-303.
773 73. Cingolani P. 2017. SnpEff v4.3T- Genomic variant annotations and functional effect
774 prediction toolbox., http://snpeff.sourceforge.net/.
775 74. Abyzov A, Urban AE, Snyder M, Gerstein M. 2011. CNVnator: an approach to
776 discover, genotype, and characterize typical and atypical CNVs from family and
777 population genome sequencing. Genome Res 21:974-84.
778 75. Team RDC. 2008. R: A language and environment for statistical computing.
779 http://www.R-project.org.
780 76. Garcia-Effron G, Park S, Perlin DS. 2009. Correlating echinocandin MIC and kinetic
781 inhibition of *fks1* mutant glucan synthases for *Candida albicans*: implications for
782 interpretive breakpoints. Antimicrob Agents Chemother 53:112-122.
783 77. Castanheira M, Woosley LN, Diekema DJ, Messer SA, Jones RN, Pfaller MA. 2010.
784 Low prevalence of *fks1* hot spot 1 mutations in a worldwide collection of *Candida*
785 strains. Antimicrob Agents Chemother 54:2655-2659.
786 78. Lackner M, Tscherner M, Schaller M, Kuchler K, Mair C, Sartori B, Istel F, Arendrup
787 MC, Lass-Flörl C. 2014. Positions and numbers of *FKS* mutations in *Candida albicans*
788 selectively influence *in vitro* and *in vivo* susceptibilities to echinocandin treatment.
789 Antimicrob Agents Chemother 58:3626-3635.
790 79. Kritikos A, Neofytos D, Khanna N, Schreiber PW, Boggian K, Bille J, Schrenzel J,
791 Mühlethaler K, Zbinden R, Bruderer T. 2018. Accuracy of Sensititre YeastOne
792 echinocandins epidemiological cut-off values for identification of FKS mutant *Candida*
793 *albicans* and *Candida glabrata*: A ten year national survey of the Fungal Infection
794 Network of Switzerland (FUNGINOS). Clinical microbiology and infection 24:1214.
795 e1-1214. e4.
796 80. Garcia-Effron G, Lee S, Park S, Cleary JD, Perlin DS. 2009. Effect of *Candida glabrata*
797 *FKS1* and *FKS2* mutations on echinocandin sensitivity and kinetics of 1,3-beta-D-
798 glucan synthase: implication for the existing susceptibility breakpoint. Antimicrob
799 Agents Chemother 53:3690-9.
800 81. Zimbeck AJ, Iqbal N, Ahlquist AM, Farley MM, Harrison LH, Chiller T, Lockhart SR.
801 2010. *FKS* mutations and elevated echinocandin MIC values among *Candida glabrata*
802 isolates from US population-based surveillance. Antimicrob Agents Chemother
803 54:5042-5047.
804 82. Prigent G, Aït-Ammar N, Levesque E, Fekkar A, Costa J-M, El Anbassi S, Foulet F,
805 Duvoux C, Merle J-C, Dannaoui E. 2017. Echinocandin resistance in *Candida* species
806 isolates from liver transplant recipients. Antimicrob Agents Chemother 61.
807 83. Park S, Kelly R, Kahn JN, Robles J, Hsu M-J, Register E, Li W, Vyas V, Fan H,
808 Abruzzo G. 2005. Specific substitutions in the echinocandin target Fks1p account for
809 reduced susceptibility of rare laboratory and clinical *Candida* sp. isolates. Antimicrob
810 Agents Chemother 49:3264-3273.
811 84. Martí-Carrizosa M, Sánchez-Reus F, March F, Cantón E, Coll P. 2015. Implication of
812 *Candida parapsilosis FKS1* and *FKS2* mutations in reduced echinocandin
813 susceptibility. Antimicrob Agents Chemother 59:3570-3573.
814 85. Jiménez-Ortigosa C, Moore C, Denning DW, Perlin DS. 2017. Emergence of
815 echinocandin resistance due to a point mutation in the *FKS1* gene of *Aspergillus*

816 *fumigatus* in a patient with chronic pulmonary aspergillosis. Antimicrob Agents
817 Chemother 61.
818
819
820
821
822

Figure 1. Schematic overview of the *in vitro* experimental evolution. A) The evolution assay: A single colony is cultured in RPMI-MOPS medium (2% glucose) for 24h at 37°C after which a standardized inoculum (10^6 cells) is resuspended in medium containing no drug (control), the drug at a concentration of 2xMIC_{50}, 1xMIC_{50} and 0.5xMIC_{50} (shown here) of the particular starting strain. Daily, the culture is re-diluted (1/10) in fresh RPMI-MOPS medium (2% glucose) with a concentration of drug based on the OD_{600} of the control culture. All strains were evolved in triplicate. Daily aliquots of evolving populations were stored in RPMI-MOPS medium containing 25% glycerol at -80°C for later examination. **B)** Ancestry of the five evolved strains that were sequenced. WGS was performed on a single colony. The name of each strain represents the experimental treatment (letter) and day of isolation (number), respectively.

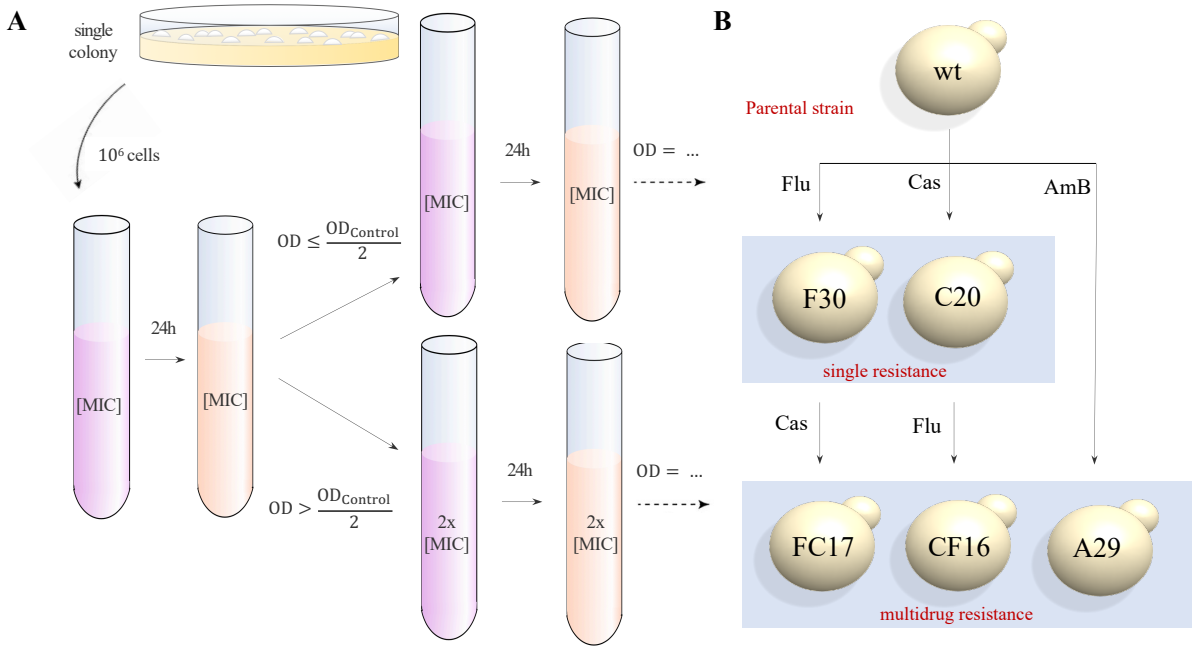

836 **Figure 2. Resistance profiles of evolved strains. A)** Summary of MIC_{50} values and associated
837 mutations/CNVs for each end-point strain and divergent intermediate strain. **B-D)** Growth profiles of
838 evolved strains relative to the wild type strain (wt) in a BDA of fluconazole **(B),** caspofungin **(C)** and
839 amphotericin B **(D)** respectively. Percentage of growth was calculated from growth without drug and
840 based on OD_{600} measurements after 48h of incubation. Each data point and its standard deviation is
841 calculated from 3 biological repeats, each represented by the mean of 2 technical repeats. Pdup: partial
842 duplication, dup: duplication

A

strain	drug	change	MIC$_{50}$ (µg/ml) Flu	Cas	AmB
wt	-	-	1	0.125	0.5
A21	AmB	*ERG3*^{W182*};*ERG11*^{E429*}	>64	-	2
A27	AmB	*ERG3*^{W182*};*ERG11*^{E429*};*MEC3*^{A272V}	>64	-	4
A29	AmB	*ERG3*^{W182*};*ERG11*^{E429*};*MEC3*^{A272V};*FLO8*^{Q384*}	>64	0.125†	4
F13	Flu	*TAC1b*^{FS191S}	32	-	-
F30	Flu	*TAC1b*^{FS191S}; Chr1^{Pdup}	>64	0.125†	1
FC16	(Flu -) Cas	*TAC1b*^{FS191S}; Chr1^{Pdup};*FKS1*^{FL635L};*CIS2*^{A27T}	>64	>64	-
FC17	(Flu -) Cas	*TAC1b*^{FS191S};Chr1^{Pdup};*FKS1*^{FL635L};*CIS2*^{A27T};*PEA2*^{D367V}	>64	>64	1
C3	Cas	*FKS1*^{FL635L}	-	64	-
C15	Cas	*FKS1*^{FL635L};*FKS1*^{M690I}	-	64	-
C20	Cas	*FKS1*^{FL635L};*FKS1*^{M690I};*ERG3*^{L207I}	0.5†	>64	0.5†
CF16	(Cas -) Flu	*FKS1*^{FL635L};*FKS1*^{M690I};*ERG3*^{L207I};Chr5^{dup}	16	64	0.5†

† see BDA graphs in supplementary figure S1

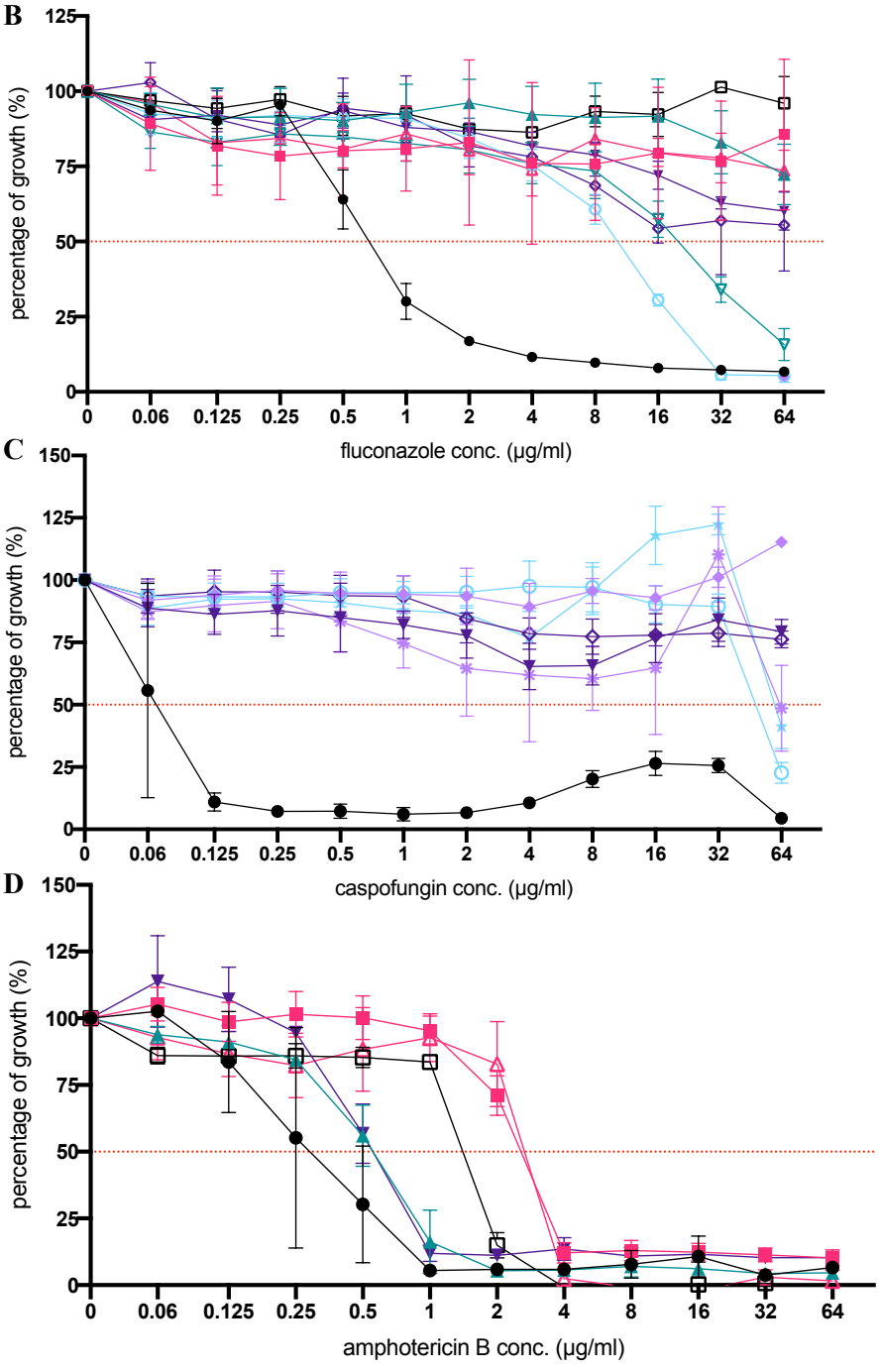

844 **Figure 3. Hotspot (HS) region mutations of the *FKS* genes that confer echinocandin resistance.**
845 Amino acid sequence of hotspot 1, 2 and 3 (HS1-3 resp.) of *C. auris* and other fungi are aligned along
846 with all mutations found to decrease echinocandin susceptibility as described in literature (references
847 are given between brackets). Species specific polymorphisms of HS are indicated in grey, the mutations
848 found to confer echinocandin resistance in this study are indicated by a grid. Δ: deletion, *: nonsense
849 mutation

	HS1	HS3	HS2	Ref
C. auris	635 F L T L S L R D P Δ P[2] Y[1] Y[2] L[1] F[2]	686 L D T Y M W Y I I C N I	1351 W I R R	[1](20) [2](10)
C. albicans[a]	641 F L T L S L R D P L[3] P[3] G[5] Y[3] H[3] S[3] Y[3] L[5] Y[4] F[3]	692 L D T Y M W Y I I C N	1358 W I R R H[3] G[6]	[3](77) [4](78) [5](79) [6](80)
C. glabrata (*FKS1*)	625 F L I L S L R D P S[7] P[7] G[7] E[7] Y[7]	676 L D T Y L W Y I V V N	1341 W V R R	[7](81)
C. glabrata (*FKS2*)[b]	659 F L I L S L R D P Δ[7] W[4] P[7] G[7] T[7] V[7] A[9] E[7] H[8] S[7] Y[8]	710 L D T Y L W Y I V V N	1375 W I R R L[8] *[8]	[8](82) [9](83)
S. cerevisiae	639 F L V L S L R D P I[10] K[10] Y[10]	690 L D T Y L W Y I I V N L[11] N[11] F[11] C[11] F[11]	1354 W V R R S[10]	[10](84) [11](29)
C. parapsilosis[c]	652 F L T L S L R D A[12]	703 L D T Y L W Y I I C N	1370 W I R R	[12](85)
C. dubliniensis	641 F L T L S L R D P P[9]	692 L D T Y M W Y I I C N	1358 W I R R	[9](83)
A. fumigatus	691 F L T L S F K D P S[13]	743 L D S Y L W Y I I C N	1403 W V N R	[13](86)

850
851 [a] Mutations R647G and P649L were exclusively heterozygous.
852 [b] *FKS2* and *FKS1* are functionally redundant in *C. glabrata* and both mutated in echinocandin resistant isolates.
853 [c] The naturally occurring alanine at position 660 allows intrinsic reduced echinocandin susceptibility in *C. parapsilosis*.
854
855

856 **Figure 4. Growth curves of end-point evolved strains.** Growth curves were plotted based on culture
857 density (spectrophotometric quantification of OD_{600} see method section) over 72h of incubation in
858 RPMI-MOPS medium containing **A)** 0.2% glucose and **B)** 2% glucose at 37°C**.** Data points are average
859 values of three biological repeats represented each by the average of two technical repeats.

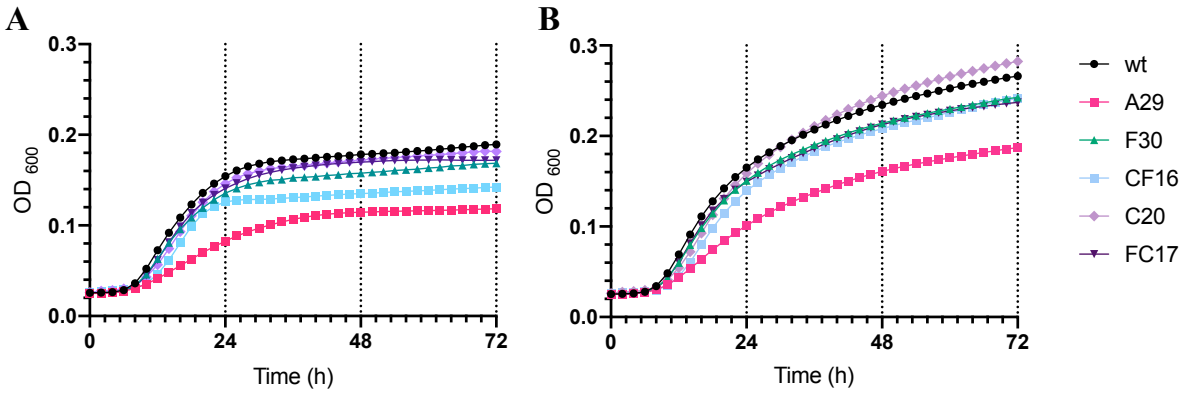

860
861
862

863 **Figure 5. Relative expression of various genes of interest among evolved strains.** Fold
864 change of expression levels for *CDR1, CDR2, ERG11* and *TAC1b* for the wild type (wt), end-
865 point evolved strains (A29, F30, FC17, C20, CF16) and intermediate strains F12 and F13 (for
866 *CDR1* and *ERG11*). Bars represent log_2-transformed means with standard deviation
867 accounting for data obtained from 3 biological repeats, each represented by the mean of 2
868 technical repeats. Asterisks indicate significant overexpression:
869 **P≤0.05;**P≤0.01;***P≤0.001;****P≤0.0001*

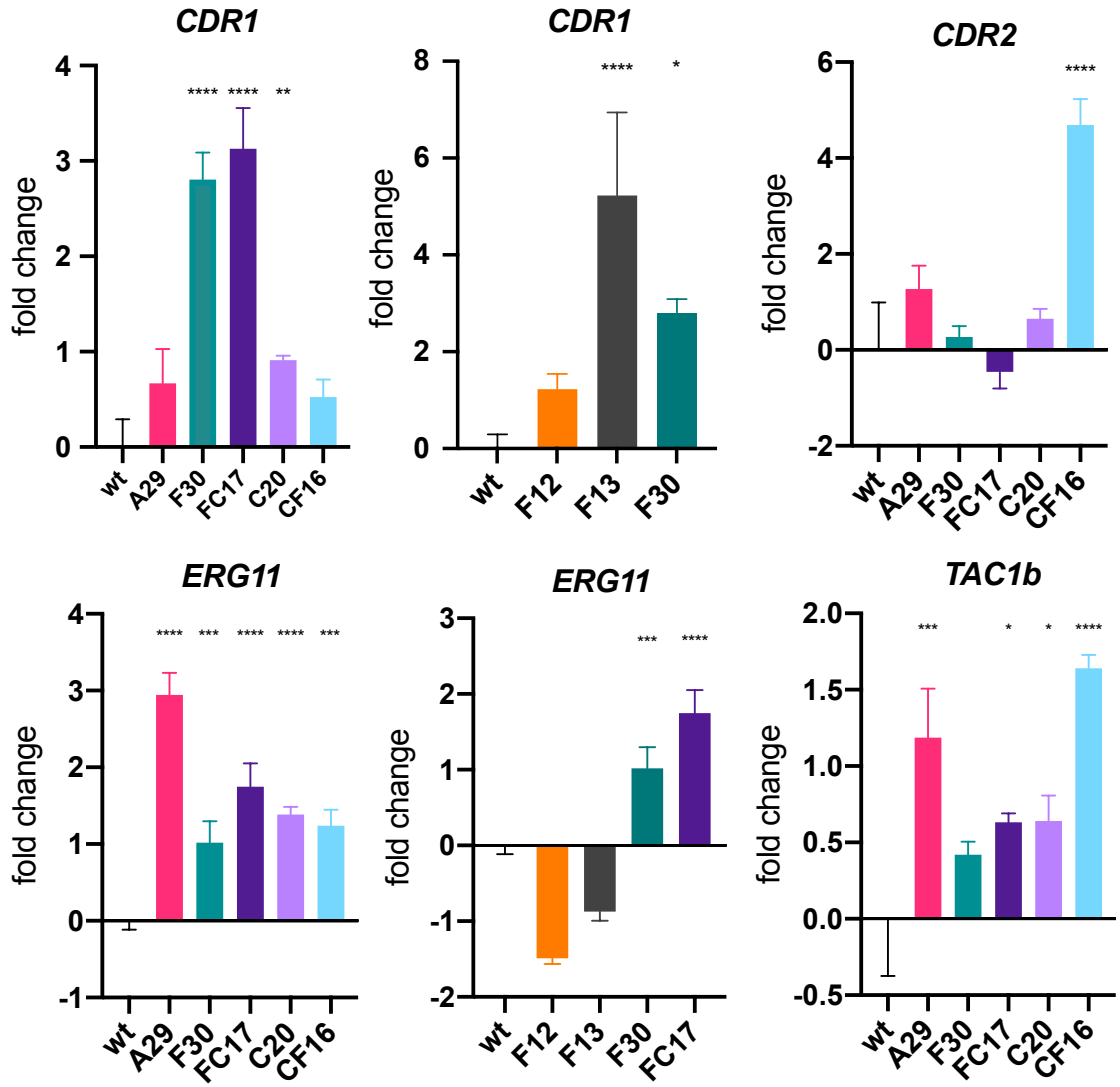

870
871

872 **Figure 6. Coverage plot of whole genome sequencing of end-point evolved strains.** The coverage
873 displayed is calculated by normalizing the average coverage depth per 5kb window. Each color
874 represents 1 chromosome (f.l.t.r.: chromosome 1 to 7). Indicated are the significant duplication in
875 chromosome 1 (Chr1) in strain F30 and FC17 and chromosome 5 (Chr5) in strain CF16. Anomality's
876 in Chr5 (spike in all strains) and Chr6 (decreased coverage) are caused by ribosomal DNA (rDNA)
877 and unambiguous mapping, and can thus be ignored.
878

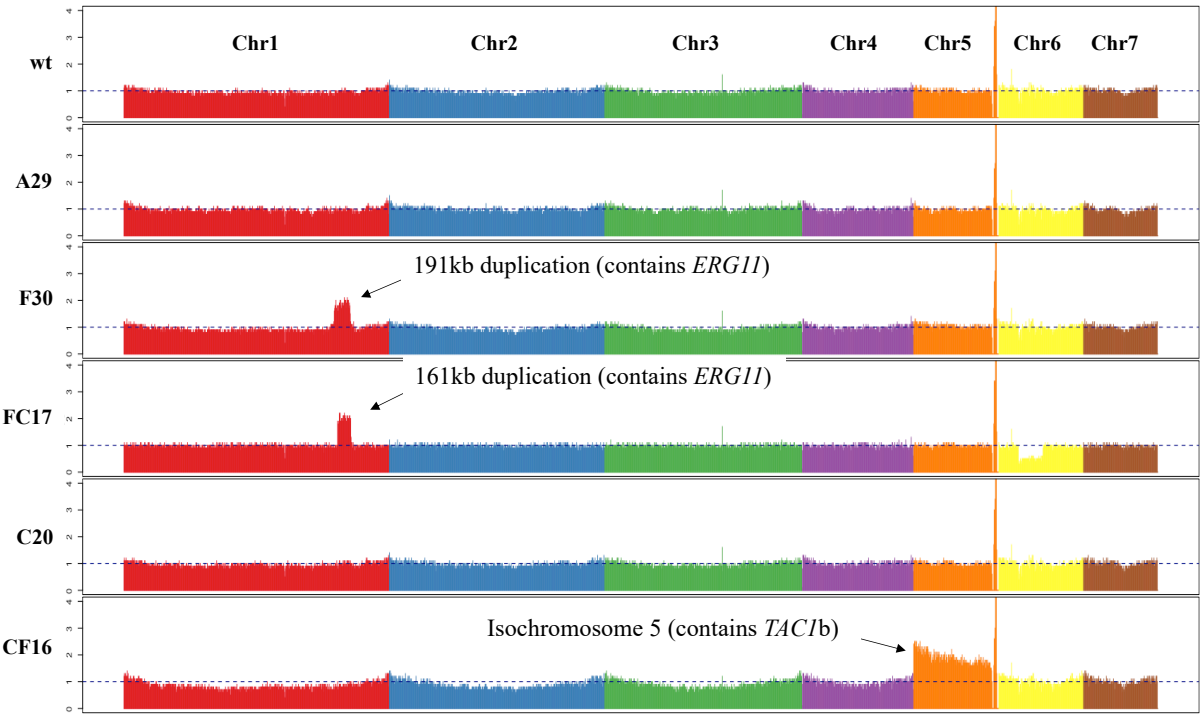

879
880
881

882 **Table 1. All non-synonymous mutations identified in the end-point evolved strains.**
883 Nucleotide and amino acid changes, as compared to the reference parent strain genome (wild
884 type) are displayed. Genes were identified based on orthologues annotated in the *C. auris*
885 B8441 genome sequenced as provided at http://www.candidagenome.org/
886

strain	change	type of change	Gene ID (B11220)	Gene ID (B8441)	Ortholog
A29	tgG/tgA|W182*	nonsense	CJI96_002270	B9J08_003737	*ERG3*
	Gag/Tag|E429*	nonsense	CJI96_001197	B9J08_001448	*ERG11*
	Cag/Tag|Q384*	nonsense	CJI96_001121	B9J08_000401	*FLO8*
	gCg/gTg|A272V	missense	CJI96_001637	B9J08_003102	*MEC3*
F30	ttcagt/agt|FS191S	codon deletion	CJI96_004335	B9J08_004820	*TAC1b*
FC17	ttcagt/agt|FS191S	codon deletion	CJI96_004335	B9J08_004820	*TAC1b*
	ttcttg/ttg|FL635L	codon deletion	CJI96_001351	B9J08_000964	*FKS1*
	gAt/gTt|D367V	missense	CJI96_001286	B9J08_001356	*PEA2*
	Gca/Aca|A27T	missense	CJI96_001769	B9J08_003232	*CIS2*
C20	atG/atA|M690I	missense	CJI96_001351	B9J08_000964	*FKS1*
	ttcttg/ttg|FL635L	codon deletion	CJI96_001351	B9J08_000964	*FKS1*
	Cta/Ata|L207I	missense	CJI96_002270	B9J08_003737	*ERG3*
CF16	atG/atA|M690I	missense	CJI96_001351	B9J08_000964	*FKS1*
	ttcttg/ttg|FL635L	codon deletion	CJI96_001351	B9J08_000964	*FKS1*
	Cta/Ata|L207I	missense	CJI96_002270	B9J08_003737	*ERG3*

887
888

Figure S1. Resistance profiles of end-point evolved strains. A-C) Growth profiles in a BDA of the end-point evolved strains (A29, F30, FC17, C20, CF16) and control strain (wt) for fluconazole **(A)** caspofungin **(B)** and amphotericin B **(C)** respectively. Percentage of growth was calculated from growth without drug and based on OD_{600} measurements after 48h of incubation at 37°C. Each data point and its standard deviation is calculated from 3 biological repeats, each represented by the mean of 2 technical repeats. **D)** Summary of MIC_{50} values for each strain and indication of (relatively low ⬆/high ⬆⬆) increase or decrease (⬇) in MIC in respect to parental strain (wt) MIC.

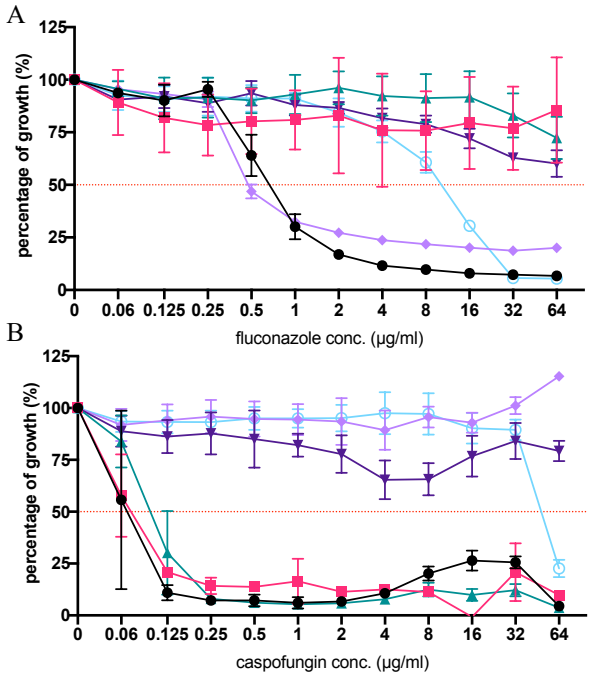

D

strain	drug	MIC_{50} (µg/ml) Flu	Cas	AmB
wt	-	1	0.125	0.5
A29	AmB	>64 ⬆⬆	0.125	4 ⬆⬆
F30	Flu	>64 ⬆⬆	0.125	1 ⬆
FC17	Flu - Cas	>64 ⬆⬆	>64 ⬆⬆	1 ⬆
C20	Cas	0.5 ⬇	>64 ⬆⬆	0.5
CF16	Cas – Flu	16 ⬆	64 ⬆	0.5

899 **Figure S2. An example of the temperature specificity range of allele-specific primers.** Here a
900 temperature gradient PCR was performed using the *MEC3* allele-specific primers (shown in
901 supplementary table S1) on gDNA of the wild type strain (wt) and strain A29, containing the
902 gCg/gTg|A272V mutation in *MEC3* (see Table 1). Primer pairs '*WT*' and 'Δ' indicate the primers
903 targeting the wild type allele (*CauMEC3_B11220_PCR/Seq1_F* and *CauMEC3_SNP_A272A_R*) and
904 mutated allele (*CauMEC3_B11220_PCR/Seq1_F* and *CauMEC3_SNP_A272V_R*) respectively and are
905 given in supplementary table S1. The green grid indicates a primer specific temperature range (63-64°C
906 resp.)

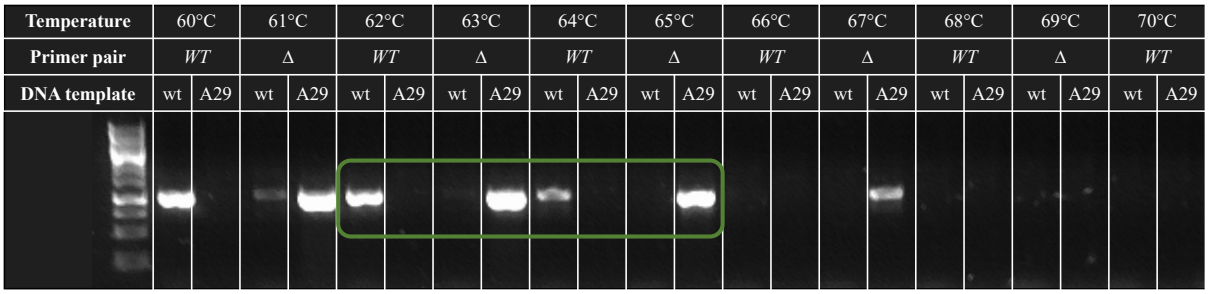

907
908
909

910 **Figure S3. Copy number variation quantification** of *TAC1b* (marker on the Chr5 duplication
911 in CF-lineage, see figure 6), *ERG11* (marker on the segmental duplication of Chr1 in F- and
912 FC-lineage, see figure 6) and *ACT1* (reference) by qPCR on gDNA. CNVs were determined
913 for 1 biological repeat represented by 3 technical repeats.

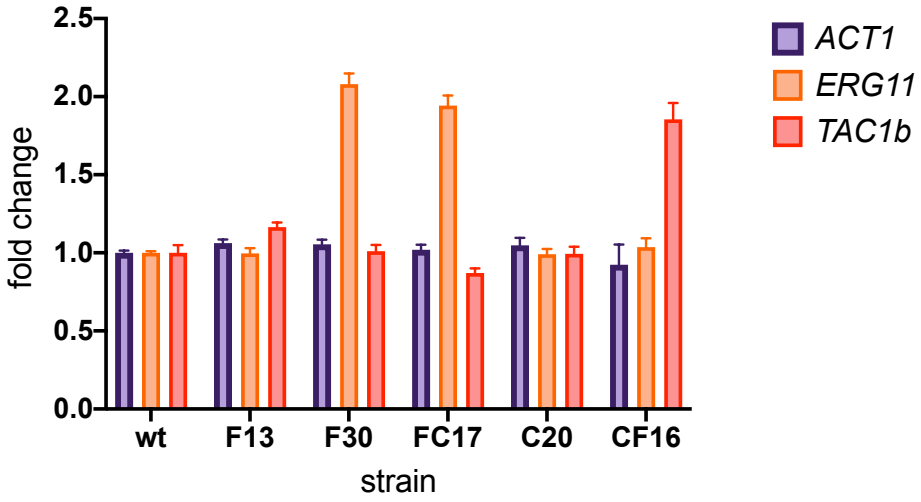

914
915
916

Table S1. All primers used in this study. Primers are arranged per marker. 'Purpose' indicates whether the primer was used for PCR and sequencing (PCR/seq), CNV or expression analysis (qPCR) or allele-specific PCR (AS). Primer pairs for AS-PCR consist of a universal PCR-sequencing primer (indicated by 'PCR/seq/AS') or universal AS-primer (indicated by 'AS') and one allele-specific primer (indicated by 'AS-wt' for the wild type allele and 'AS-mt' for the mutant allele).

Marker	Purpose	Primer name	Sequence (5'-3')
TAC1b	PCR/seq/AS	CauTAC1b_B11220_PCR/Seq3_F	CGCTGCTCAAGTCAGGTAAGG
	PCR/Seq	CauTAC1b_B11220_Seq3_R	AGGTGGCAAAGAAAGTCAACATG
	AS-wt	CauTAC1b_SNP_F15F_R	CAATCCACTCAATACTTTGCGTATTG
	AS-mt	CauTAC1b_SNP_F15/_R	TCAATCCACTCAATACTTTGCGTATTA
	qPCR	CauQ-TAC1B-F1	CACGCCCAATGGTTCGC
	qPCR	CauQ-TAC1B-R1	GGGTGAAGGTGCCTCCATG
PEA2	PCR/seq/AS	CauPEA2_B11220_PCR/Seq1_F	TAACACCTCGCCTAACTTGTGGT
	PCR/seq	CauPEA2_B11220_Seq1_R	CTTTTCTCCCACATTGCATC
	AS-wt	CauPEA2_SNP_D367D_R	GCAGAGTACCGTCTAGCATTAAATGA
	AS-mt	CauPEA2_SNP_D367V_R	GCAGAGTACCGTCTAGCATTAAATGT
MEC3	PCR/seq/AS	CauMEC3_B11220_PCR/Seq1_F	CCAATGGGTATCATAAGTCAGCG
	PCR/seq	CauMEC3_B11220_Seq1_R	GTATAACACCTCGACATCA
	AS-wt	CauMEC3_SNP_A272A_R	GTGCTAACGATTTTCGGCG
	AS-mt	CauMEC3_SNP_A272V_R	ACGTGCTAACGATTTTCGGCA
FLO8	AS	CauFLO8_SNP_Seq_R	GTGGACAGACACAGCTTGCTG
	AS-wt	CauFLO8_SNP_Q384Q_F	GAACATGGGTATGCCTCGGC
	AS-mt	CauFLO8_SNP_Q384*_F	ATGAACATGGGTATGCCTCGGT
	PCR/seq	CauFLO8_B11220_Seq1_R	GTGGACAGACACAGCTTG
	PCR/seq	CauFLO8_B11220_Seq1_F	AGTTCCCTCTTGATCAGA
FKS1	PCR/seq	CauFKS1_B11220_Seq2.2_F	ATTTCAGAAGGAACCTGG
	PCR/seq	CauFKS1_B11220_Seq2.2_R	CGTTCCATTCGCTTATTC
	AS	CauFKS1_B11220_Seq2_F	CTGCGAAATCAACACCTTTG
	AS-wt	CauFKS1_SNP_M690M_R	CTTGTTCTTCTTGGATACTTACGTG
	AS-mt	CauFKS1_SNP_M690I_R	GTTCTTGTTCTTCTTGGATACTTACGTA
	AS-wt	CauFKS1_SNP_FL635FL_R	GTTGGCCGAATCTTACTTCCTC
	AS-mt	CauFKS1_SNP_FL635L_R	GTTGGCCGAATCTTACTTCCTG
ERG3	PCR/seq	CauERG3_Seq2_F	TCAACGGATTCTCCAAGC
	PCR/seq	CauERG3_B11220_Seq5_R	TGGAACCATCCGTCAACTG
	AS^{L207}	CauERG3_PCR/Seq4_R	TACCATTGAATTTGGCTGC
	AS-wt	CauERG3_SNP_L207L_F	CATCTACTTCATCCACCGCTAGC
	AS-mt	CauERG3_SNP_L207I_F	GCATCTACTTCATCCACCGCTAGA
	AS^{W182}	CauERG3_B11220_PCR/Seq1_F	CTCGTTTAGAGCTCGTTTTCAG
	AS-wt	CauERG3_SNP_W182W'_R	GGAACTGTAACAATACGGCTCTC
	AS-mt	CauERG3_SNP_W182*'_R	GGAACTGTAACAATACGGCTCTT
ERG11	PCR/seq	CauERG11_ Seq2_F	AACGAGAGAAGAAAGACCG

	PCR/seq/AS	CauERG11_ B11220_PCR/Seq4_R	GCTGGTTTGGTGAAGAATTCGG
	AS-wt	CauERG11_SNP_E429E_F	CCCACACAGATGGGGCG
	AS-mt	CauERG11_SNP_E429*_F	GACCCACACAGATGGGGCT
	qPCR	CauQ-ERG11-F	GTTTGCCTACGTGCAATTGG
	qPCR	CauQ-ERG11-R	GTAGTCGACTGGTGGAAGCG
CIS2	PCR/seq	CauCIS2_B11220_Seq3_R	TTGTCTCGTTCTGCTTCCA
	PCR/seq	CauCIS2_B11220_PCR/Seq3_F	TTTTTTCGCACCCATTTCG
	AS	CauCIS2_B11220_Seq2_R	GCGGTGAGCTGAAAGAGAGC
	AS-mt	CauCIS2_SNP_A27T_F	CGGCCATGGAGAACCA
	AS-wt	CauCIS2_SNP_A27A_F	CGGCCATGGAGAACCG
ACT1	qPCR	CauQ-ACT1-F	GAAGGAGATCACTGCTTTAGCC
	qPCR	CauQ-ACT1-R	GAGCCACCAATCCACACAG
LSC2	qPCR	CauQ-LSC2-F	TGTACCGACATGGAAGGAATTG
	qPCR	CauQ-LSC2-R	TCACACCAAGACAGCTTTATCC
UBC4	qPCR	CauQ-UBC4-F	ACCTCAGCGGTTAACAAGAG
	qPCR	CauQ-UBC4-R	CGAATCGGTGACGATCCATTA
CDR1	qPCR	CauQ-CDR1-F	GAAATCTTGCACTTCCAGCCC
	qPCR	CauQ-CDR1-R	CATCAAGCAAGTAGCCACCG
CDR2	qPCR	CauQ-CDR2-F	GTCAACGGTAGCTGTGTG
	qPCR	CauQ-CDR2-R	GTCCCTCCACCGAGTATGG